Assessing Lung Vasculature Development and Application to Early Preterm Gestation Patients

Randi Dias, Aren Singh Saini, & Walter O'Dell
Departments of Radiation Oncology and Biomedical Engineering, University of Florida, Gainesville, FL

I. INTRODUCTION

- The hindered development in a preemie infant's lungs can lead to severely inadequate gas exchange, which contributes to lung failure being the leading cause of neonatal mortality[1]
- In preemies, obstructive lung diseases are commonly seen due to reasons such as lung underdevelopment, oxygen therapy, and ventilator support. In adults who were born prematurely, decreased lung function has been observed, although they previously did not display significant respiratory disease as neonates[2]
- Improved standardized methods are needed to achieve and measure reliable, non-invasive, and quantitative assessment of lung development in preemies

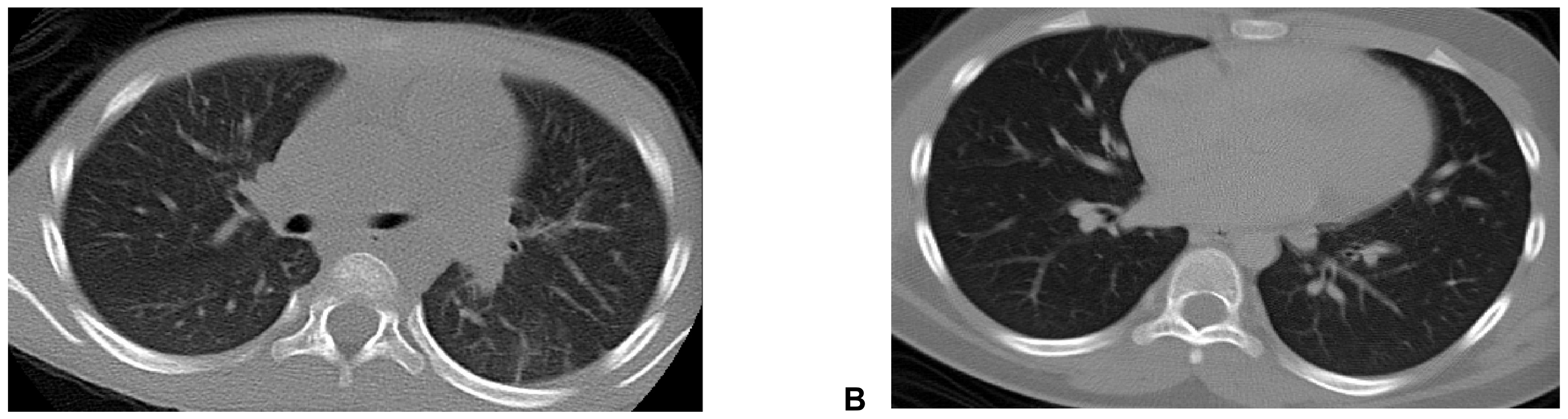

Figure 1: Representative changes in pediatric lung CT appearance with age. [Left] shows a CT chest image of a 5-year old prematurely-born child. [Right] The same child's lung CT scan at 9 years of age, displaying lung and body growth over time.

Objective: collect quantifiable data and establish procedures that can provide clinical guidance to improve the mortality and quality of life of prematurely born infants, and provide better care as these children advance onto their adult lives

II. METHODOLOGY: IMAGING AND SKELETONIZATION

CHEST CT IMAGE ACQUISITION and LUNG VOLUME SEGMENTATION[3]

- Lung CT scans at 1 week to 20 years of age were retrospectively gathered within an IRB-approved protocol for 30 preemie and 30 full-term patients up to 18 years of age that were seen at the UF Health Shands Pediatric Pulmonary Care Center from 2014-2019.
- In-house software built upon the NIH ImageJ platform was used to automatically segment the lung volume (Fig 2A), extract the pulmonary vessel trees, and characterize the radius and length of each vessel branch.
- To-date, this approach was applied to the right-hemi-lung of 16 adolescents from 2 to 19 years of age. 8 males and 8 females were analyzed and compared, 9 of which were full term while the other 7 were preemies. Each subject provided 3-7 follow-up scans.
- For each subject, gestational age, sex, and presence of infection/disease were recorded to compare and analyze the subject factors later in the study.
- Calibration curves were used to adjust for variances in imaging parameters, pixel size, and reconstruction filters

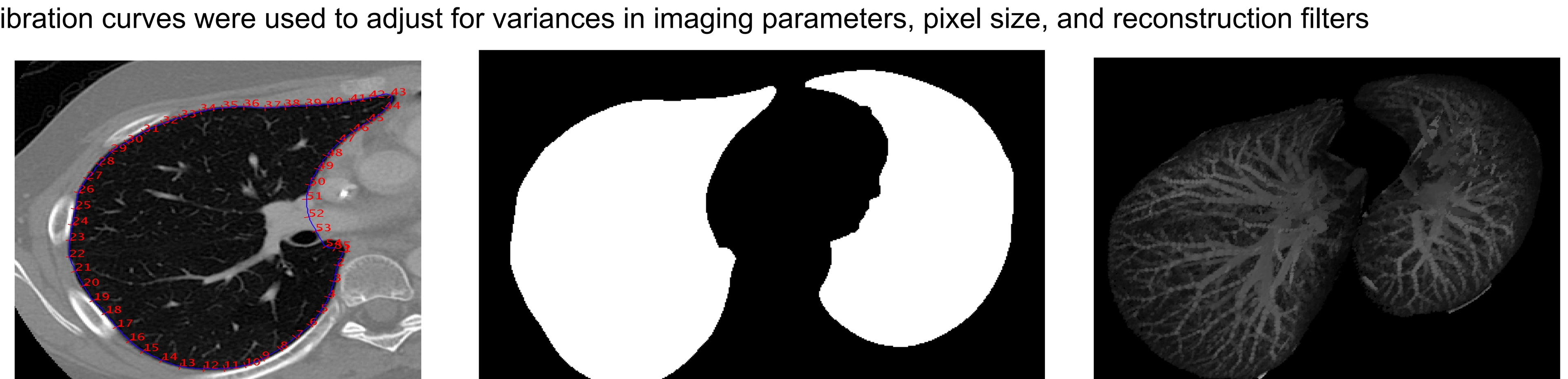

Figure 2: 3D CT datasets and lung volume segmentation. Image [A] shows a pediatric patient's representative chest CT scan with a snake (blue contour with red node points) used to segment the right hemi-lung volume. [B] displays the lung mask on this same slice obtained after contouring all the segmented slices across both hemi-lungs. [C] displays the 3D maximum-intensity projection (MIP) of the lung volume after stacking all segmented slices (each acquired with a 3 mm slice thickness) across both hemi-lungs.

LUNG VESSEL TREE SEGMENTATION[3]

- The major airways were segmented using a seeded region-growing method (Fig 3A) and subtracted from the lung volume images.
- The pulmonary vessels were extracted similarly using a manually-selected seed point placed in the pulmonary trunk (Fig 3B).
- Skeletonization of the tree structure was applied to facilitate traversing and labeling each branch in the tree structure (Fig 3C).
- The radius and length of each branch were then computed automatically from the branch centerline and the image 3D distance map.

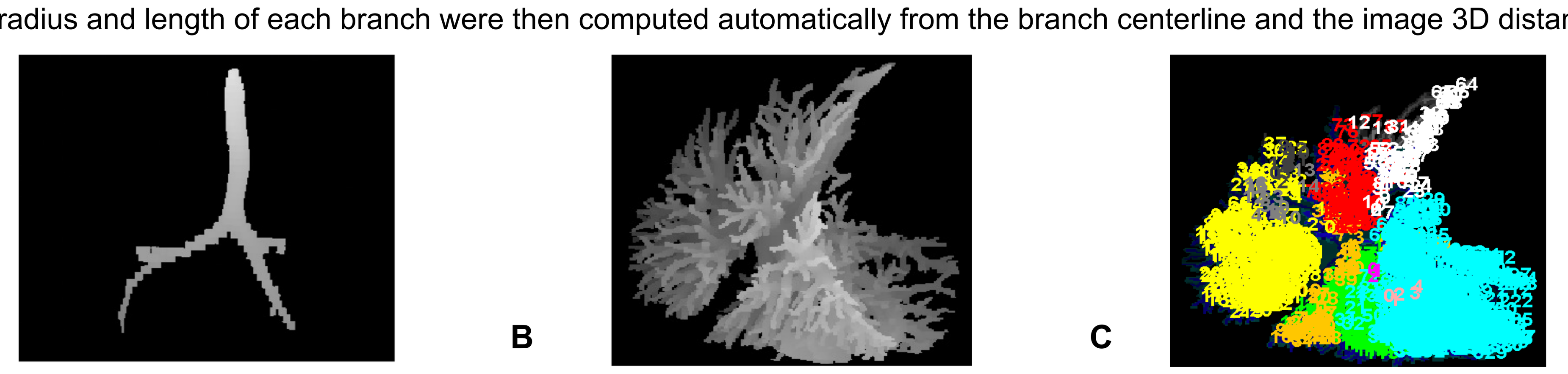

Figure 3. Airway and vessel tree segmentation, and branch labeling. [A] shows a maximal intensity projection (MIP) or the extracted airway tree [B] shows the MIP of segmented vessel tree in the same patient. Extraction of the branch centerlines (skeletonization) enables tree traversal and the identification of individual branches within each tree structure. [C] shows the number-labeled branches where each tree structure uses a unique color.

ACKNOWLEDGEMENTS

This study is funded by the UF Department of Radiation Oncology and the UF University Scholars Program.

III. RESULTS AND DISCUSSION

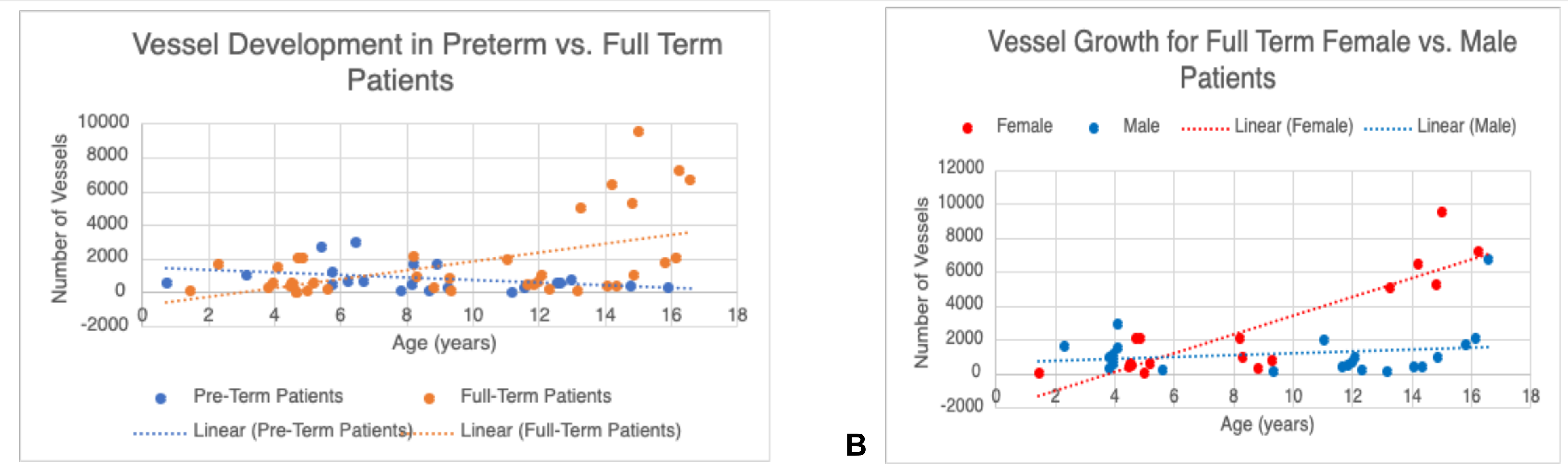

Figure 4: Number of branches versus age for pediatric subjects. [A] represents a scatter plot of vessel growth in preterm vs. full term patients as years progress. [B] represents a scatter plot of vessel growth in full term male vs. female patients as years progress.

- For full term patients, a linear regression fit to the data indicates that the number of lung vessels increases as the patient ages. However, a significant difference was not achieved (p-value of 0.074)
- A trend for a slight increase in the number of lung vessels was observed in patients, between the ages 1-6, who were born pre-term. However, there was an apparent drop in the number of lung vessels from ages 7 to 11, and then the lung vessels tended to stabilize and level off between the ages 12-16
- Between male and female subjects, there was a trend for greater increase in the number of vessels with age for females, relative to male patients (p-value of 0.15)

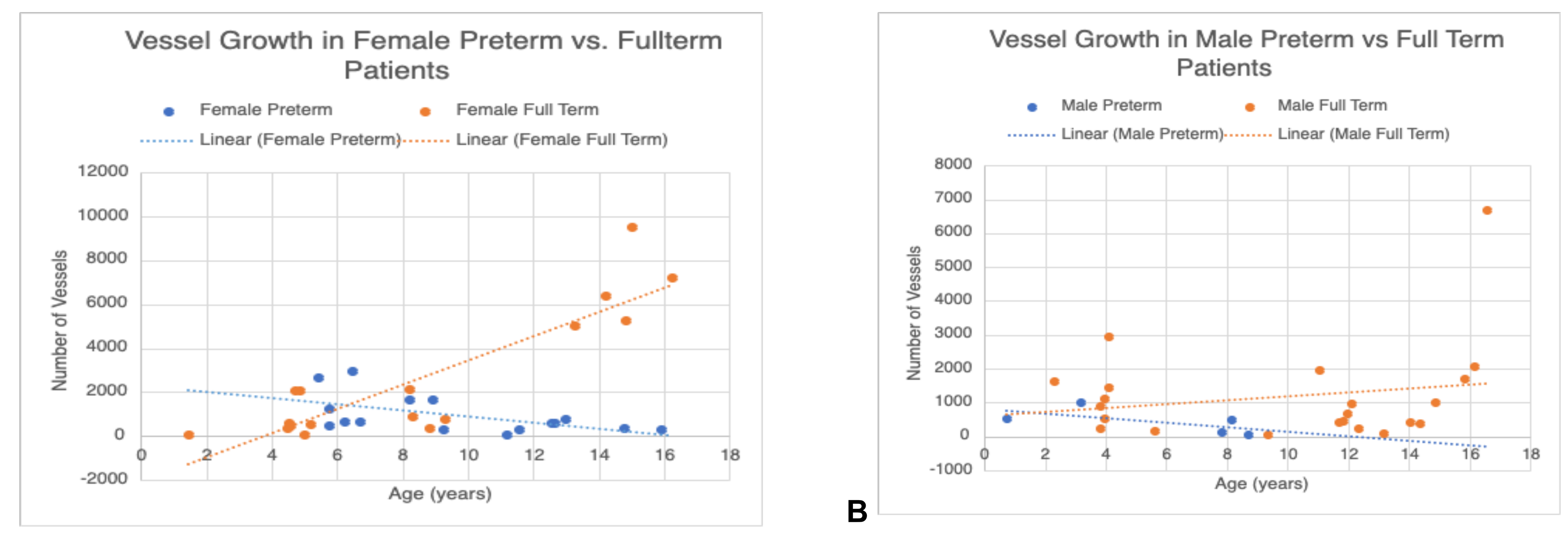

Figure 5: Plot A (left) portrays lung vasculature development over time for female preterm vs full term patients. Image B (left) portrays lung vasculature development over time for male preterm vs full term patients

- For female full-term subjects, there was a significantly larger increase in the number of branches over time (the slope of the graph of Fig 5A) compared to female preemies. A two-sample T test was performed and a p-value of 0.04 was obtained, indicating a statistical significance in the data.
- A similar trend was observed when comparing the vessel development in male preterm vs full term patients, but the difference in the slopes of the male patients (p-value 0.27) did not reach significance.
- Differences between preterm and full-term subjects in the number of vessel branches became more apparent in the teenage years than in younger children.

IV. CONCLUSIONS AND FUTURE DIRECTIONS

- A quantitative analysis of pulmonary vascular development over time was conducted to compare full-term to prematurely-born pediatrics using quantitative metrics obtained from repeat chest CT scans.
- The number of vascular branches increased with age in full-term subjects with a larger slope than for prematurely-born children
- Our preliminary data identified a significant difference in the rate of lung vascular development between females born prematurely and those born full-term, which becomes more apparent in the teenage years

Several factors that impact our ability to consistently extract vessel branches from pediatric CT scans were:

- Limited patient samples made the current analyses mostly exploratory.
- Variations in image quality, imaging parameters, CT scanner technology, and the ability of patients to remain still for a long period of time
- In these subjects, many scans exhibited acute lung infection and/or edema, which can obscure vessels in the CT image.

Plans for Future Work

- Improved calibration tools are being developed to better compare vessel metrics across patients
- Analysis of additional pediatric datasets is on-going to increase the statistical power for detecting trends and group differences
- Improve the quality and reliability of the vessel extraction algorithm to improve the reliability and scope of the vessel results.
- Correlate patterns of lung vessel development with other patients' factors (e.g., body weight and lung volume) and disease states (e.g., adult pulmonary hypertension)

IV. REFERENCES

1. Simmons, L. E., Rubens, C. E., Darmstadt, G. L., & Gravett, M. G. (2010, December). Preventing preterm birth and neonatal mortality: exploring the epidemiology, causes, and interventions. In *Seminars in perinatology* (Vol. 34, No. 6, pp. 408-415). WB Saunders.
2. Jones, M. (2009). Effect of preterm birth on airway function and lung growth. *Paediatric Respiratory Reviews*, *10*, 9-11
3. O'Dell, W. G., Gormaley, A. K., & Prida, D. A. (2017). Validation of the Gatortail method for accurate sizing of pulmonary vessels from 3D medical images. *Medical Physics*, *44*(12), 6314-6328.